physica status solidi c
www.pss-c.com
current topics in solid state physics

Photoconductivity in amorphous selenium blocking structures

A. Reznik[1], S. D. Baranovskii[2], O. Rubel[2], K. Jandieri[2], and J. A. Rowlands[1]

[1] Imaging Research, Sunnybrook Health Sciences Centre, 2075 Bayview Avenue, Toronto, M4N 3M5, Canada
[2] Department of Physics and Material Sciences Center, Philipps University Marburg, 35032 Marburg, Germany

Received 6 August 2007, revised 27 October 2007, accepted 30 October 2007
Published online 7 February 2008

PACS 71.55.Jv, 72.20.Jv, 72.20.Ht, 72.40.+w

Photoconductive properties of the first practical a-Se avalanche photosensor (hole drift mobility, photocurrent response time, quantum yield of charge photogeneration and avalanche multiplication gain) have been studied. It has been shown that hole transport and avalanche multiplication mechanisms in multilayered a-Se blocking structure used in practical photosensors are similar to those observed in a-Se monolayers confined between insulating layers and used for the first manifestation of avalanche effect in this material by Juska and Arlauskas, phys. stat. sol. (a) **59**, 389 (1980). It is suggested that combination of high avalanche gain (up to 1000) with high quantum efficiency of charge photogeneration (almost 100%) and fast photocurrent time response (~ 1 ns) makes a-Se avalanche photosensor a promising candidate to replace vacuum photomultiplier tubes for application in medical radiation imaging.

phys. stat. sol. (c) **5**, No. 3, 790–795 (2008) / **DOI** 10.1002/pssc.200777582

phys. stat. sol. (c) **5**, No. 3, 790–795 (2008) / **DOI** 10.1002/pssc.200777582

physica status solidi c
www.pss-c.com
current topics in solid state physics

Photoconductivity in amorphous selenium blocking structures

A. Reznik[*, 1], **S. D. Baranovskii**[2], **O. Rubel**[2], **K. Jandieri**[2], **and J. A. Rowlands**[1]

[1] Imaging Research, Sunnybrook Health Sciences Centre, 2075 Bayview Avenue, Toronto, M4N 3M5, Canada
[2] Department of Physics and Material Sciences Center, Philipps University Marburg, 35032 Marburg, Germany

Received 6 August 2007, revised 27 October 2007, accepted 30 October 2007
Published online 7 February 2008

PACS 71.55.Jv, 72.20.Jv, 72.20.Ht, 72.40.+w

[*] Corresponding author: e-mail alla.reznik@sunnybrook.ca, Phone: + 1 416 4806100, ext.7129, Fax: + 1 416 480 5714

Photoconductive properties of the first practical a-Se avalanche photosensor (hole drift mobility, photocurrent response time, quantum yield of charge photogeneration and avalanche multiplication gain) have been studied. It has been shown that hole transport and avalanche multiplication mechanisms in multilayered a-Se blocking structure used in practical photosensors are similar to those observed in a-Se monolayers confined between insulating layers and used for the first manifestation of avalanche effect in this material by Juska and Arlauskas, phys. stat. sol. (a) **59**, 389 (1980). It is suggested that combination of high avalanche gain (up to 1000) with high quantum efficiency of charge photogeneration (almost 100%) and fast photocurrent time response (~ 1 ns) makes a-Se avalanche photosensor a promising candidate to replace vacuum photomultiplier tubes for application in medical radiation imaging.

1 Introduction Impact ionization and avalanche formation in amorphous selenium are interesting phenom-ena which have been intriguing scientists from the 1980's when these effects first were experimentally observed [1], until very recently when they first were explained in terms of the modified lucky-drift (LD) model [2, 3]. During this 25 year period it has been shown experimentally that avalanche multiplication in a-Se starts at electric fields F_{AV} ~ 70 V/μm where hot holes gain enough energy to initiate impact ionization.

Due to the high electric fields required for holes to avalanche, the first experiments on avalanche multiplication were performed using a-Se layers sandwiched between two polyethyleneteraphalat layers [1]. These insulating layers prevented carrier injection from the electrodes and permitted high voltage biasing during photocurrent measurements. This facilitated time-of-flight (TOF) measurements at high electric fields. The quantum yield of charge photogeneration was derived by time integrating the a-Se transient photocurrent produced by single pulse illumination. These measurements demonstrated that at $F > F_{AV}$ the experimental quantum yield was significantly larger than unity and exponentially dependent on a-Se layer thickness [1, 4]. This pointed out avalanche multiplication. After each measurement the charge trapped at the a-Se/insulator inter-face was eliminated and the sample reset to its initial state by shorting the electrodes and resting the sample. Although this concept was successfully used to prove the existence of avalanche multiplication in a-Se, it is not valid for practical avalanche photodetectors where a continuous flow of current is required. For practical photodetectors an a-Se structure which provides an exit for mobile carriers from the bulk of the photoconductor directly to the electrode while preventing the injection of carriers from the electrode into the photoconductor has to be developed. Such a structure was first realized in a-Se phototargets of ultrasensitive HARP (High-gain Avalanche Rushing Photoconductor) video camera tubes. In the HARP structure a-Se layer is confined between CeO_2 and Sb_2S_3 layers, which act as blocking layers for holes and electrons, respectively: CeO_2 is an n-type wide bandgap material and prevents injection of positive charge from the anode by forming a high potential barrier to holes; the Sb_2S_3 layer contains a large number of electron traps which when filled, form a negative space-charge barrier thus stopping injection of electrons from the cathode [5]. The absence of carrier injection is confirmed by the low dark current, which after stabilization does not exceed 0.1 nA/mm^2 at any F (1-100

V/μm). Due to the avalanche gain HARP video camera tubes are characterized by very high sensitivity to light, which makes them capable of producing high quality images even at extremely low light intensities [6, 7]. Recently, it has been proposed to use HARP-like a-Se blocking structure in medical X-ray systems and for gamma-ray detectors used in PET (Positron Emission Tomography) [8, 9]. For PET a-Se avalanche photosensors are considered to be an alternative to vacuum photomultiplier tubes for detection of light emitted from scintillation crystal.

The promising medical applications motivated our study of hole transport, effective quantum efficiency and avalanche multiplication gain of a-Se HARP photosensors that are prototype structures for use in PET detectors. Hence, the evaluation of photoconductive properties has been carried out in respect to utilization in PET. Photoconductivity was studied at 420 nm wavelength of excitation which corresponds to peak emission of advanced scintillation crystals used in PET detectors. A practically useful criterion for avalanche gain optimization is suggested.

2 Experimental

2.1 HARP phototarget structure HARP phototargets with different a-Se layer thicknesses (d= 8, 15, 25 and 35 μm) are used here. The details of HARP tube design can be found in Ref. [10]. a-Se blocking structure is deposited on a glass plate with an ITO layer that serves as the transparent front positive electrode (Figure 1). The electric field across the a-Se layer is created by connecting a positive voltage supply to an ITO layer. Optical photons are absorbed at the front a-Se surface where they create electron-hole pairs. Photogenerated electrons are immediately captured by the adjacent positive electrode while holes are drawn across the a-Se layer to the free surface (i.e. cathode) under the influence of the applied field. When HARP camera is operated in the avalanche regime a bias field in excess of the hole avalanche multiplication threshold F_{AV} is applied to the target and accelerated photogenerated holes undergo avalanche multiplication through multiple impact ionization collision events. The holes accumulate at the free surface and form a charge image. As the electron beam scans the free surface and resets the accumulated charge, a current proportional to the amount of accumulated charge at the scan spot is detected (Fig. 1).

2.2 Hole mobility For mobility measurements light from a pulsed nitrogen laser beam (337.1 nm, 800 ps, 1.65 mJ) was incident on the front positively biased surface of the a-Se layer (8 μm thick) of HARP tube and charge transport was monitored using TOF technique. Due to the high absorption coefficient of a-Se at 337 nm, carriers are generated at the surface of the sample, so holes traverse a distance equal to d. The duration of the laser pulse was shorter than the transit time for holes under all our experimental conditions. All TOF traces were recorded on a 2.5 GHz bandwidth digital oscilloscope. To prevent accumulation of holes, the back of the target is discharged by a scanning electron beam.

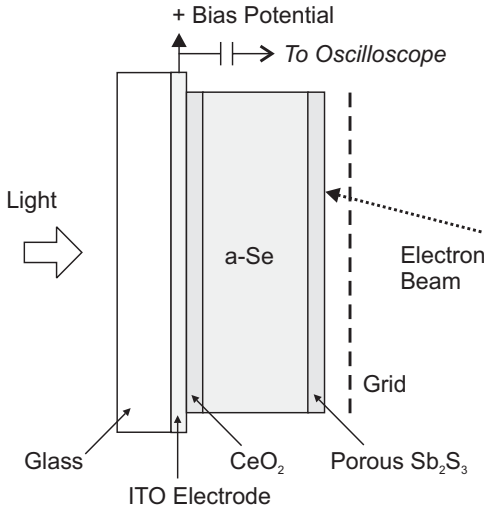

Figure 1 Schematic presentation of the structure of a-Se multilayered HARP phototarget.

TOF measurements were performed at steady state temperatures between ~25 °C and 40 °C. Conditions above room temperature were produced via external heating of the a-Se target with hot air passed into the camera enclosure. The possible crystallization of a-Se at elevated temperature dictated the upper bound of the temperature range.

Figures 2 and 3 show transient current pulses at sub-avalanche ($F < F_{AV}$) and avalanche regimes ($F > F_{AV}$), respectively.

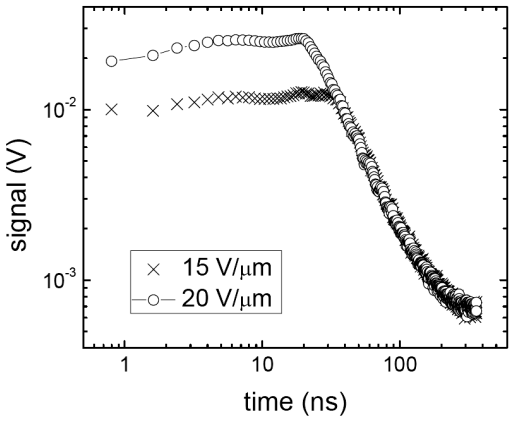

Figure 2 Room temperature hole transient photocurrent pulses.

As it is seen from Fig. 2 the transient profile is quasi-rectangular where the photocurrent rises rapidly then remains approximately constant at a plateau until the majority of mobile holes have reached the back of the layer when it falls precipitously. The hole transit time t_h is defined as the time at which the magnitude of the photocurrent falls to half the nominal value of the plateau.

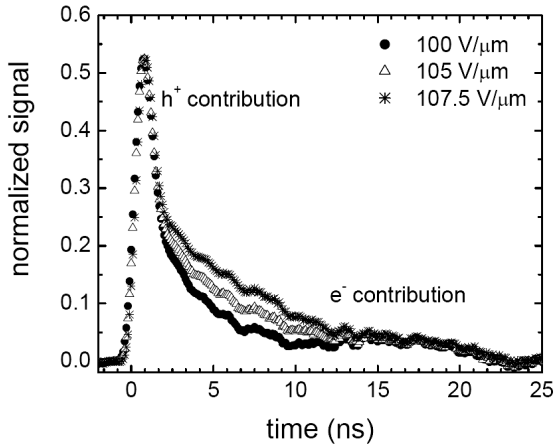

Figure 3 Room temperature transient photocurrent pulses in a-Se layers of HARP phototarget at F > F_{AV} (avalanche regime).

the avalanche regime (Fig. 3) the shape of the TOF signal is dramatically different from that at lower fields. It consists of a rapid burst due to the avalanching hole contribution and comparatively long tail due to the contribution of electrons which are created in the bulk of the a-Se as a result of impact ionization and travel towards the positive electrode. To derive t_h at the avalanche regime TOF curves were de-convolved in Matlab with the known shape of the laser pulse.

Drift hole mobility is then obtained from $\mu = d/t_h F$ and is shown in Fig. 4. It was found that mobility has thermally activated behavior with field dependent activation energy ε_a : ε_a decreases with increase in F and vanishes at ~ 50 V/μm (see Fig. 5).

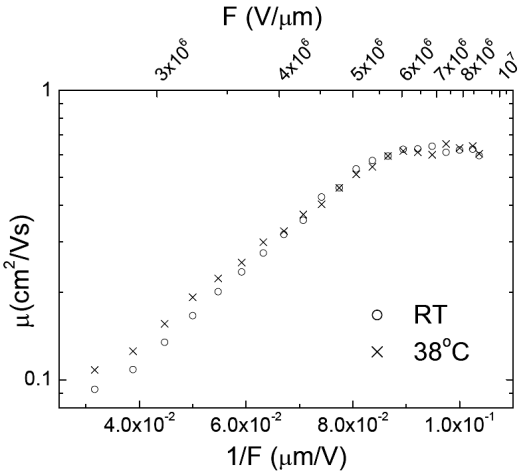

Figure 4 Field dependencies of hole mobility in a-Se HARP layers at room temperature (RT) and at slightly elevated temperature.

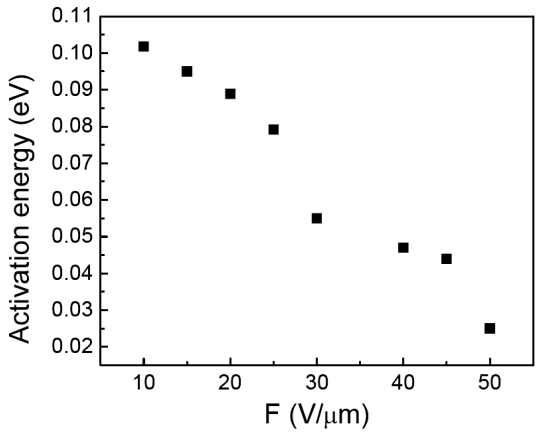

Figure 5 Field dependence of the activation energy of hole mobility a-Se HARP layers.

2.3 Quantum yield, avalanche gain and breakdown field measurements Quantum yield η^* of photogeneration was measured for λ=420 nm using a-Se phototargets of HARP tubes with d= 8, 15, 25 and 35 μm at constant light intensity I. η^* refers to the superposition of the primary mechanism by which electron-hole pairs are generated and the secondary mechanism by which holes avalanche [3].

The details of the experimental apparatus used can be found in Ref. [11]. η^* for different d was calculated using experimentally measured photocurrent S [11] by the following expression:

$$\eta^* = \frac{S/e}{IT/h\nu} \tag{1}$$

where e is the elementary charge, $h\nu$ is incident photon energy, T is the transmission through the layers in front of the a-Se. Thus calculated η^* is shown in insert to Fig. 6 as a function of F for d=8 μm.

As it is shown in the insert to Fig. 6 in the non-avalanche regime (F < 70 V/μm) η^* is close to unity even at comparatively low electric fields. Above the avalanche threshold of 70 V/μm η^* increases rapidly with further increase in electric field since avalanche charge begins to contribute to the photocurrent. Since η^* is not significantly varying below F_{AV}, the avalanche gain g_{av} can be calculated by the following relationship

$$g_{av}(F) = \eta^*(F) / \eta^*_{70V/\mu m} \tag{2}$$

where $\eta^*_{70V/\mu m}$ is η^* at F=70 V/μm. Figure 6 shows g_{av} for d= 8, 15, 25 and 35 μm. The sharp increase in g_{av} above 70 V/μm is obvious.

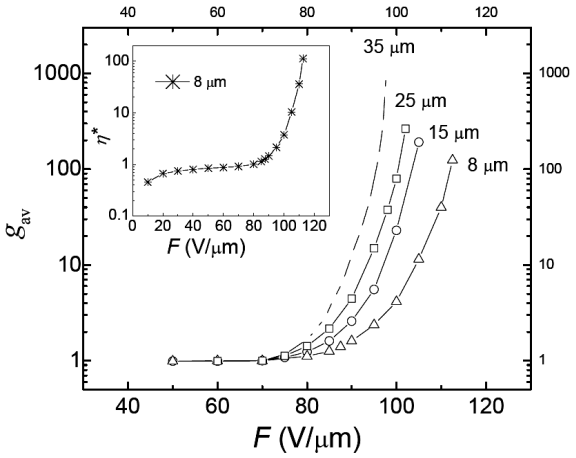

Figure 6 Field dependence of the a-Se HARP gain g_{av} under constant illumination at 420 nm for different photosensitive layer thicknesses. Insert shows field dependence of the quantum yield for 8 μm thick a-Se layer as derived from the measured photocurrent by Eq. (1).

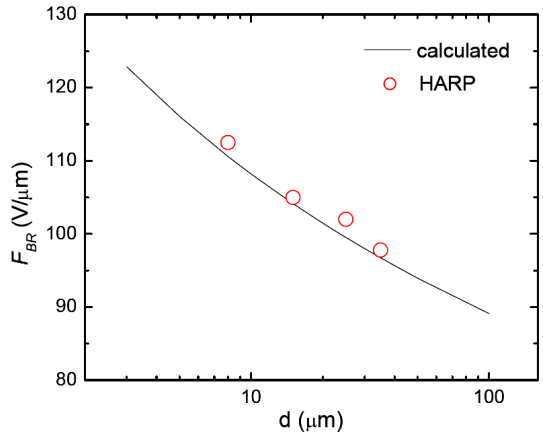

Figure 7 The dependence of the breakdown threshold on a-Se layer thickness. Symbols-experimental results, line – calculation in accordance with Eq. (4).

F_{MAX} of the a-Se was determined as the electric field at which the breakdown noise exceeding hole avalanche noise first appears [12]. The results for different a-Se thicknesses d are shown in Fig. 7 (open circles).

3 Results and discussion The experimental results on charge transport and effective quantum efficiency of charge photogeneration in a-Se blocking structures of HARP targets agree well with the theory of avalanche multiplication in a-Se [2, 13] and previous studies [1, 4, 14] that showed avalanche multiplication in a-Se at electric fields in excess of 70 V/μm when drifting holes gain sufficient energy from the field to initiate impact ionization process. It should be noted that the presence of blocking layers for holes and electrons does not affect the hole transport mechanism. In the sub-avalanche regime transport remains non-dispersive like in a-Se monolayers investigated previously [14]. Indeed, the existence of a plateau in the photocurrent profile (Fig. 2) followed by an abrupt decrease in signal magnitude indicates that hole transport is non-dispersive for the applied temperatures.

The fact that the activation energy of hole mobility decreases with field to the experimentally undetectable value at ~ 50 V/μm (Fig. 5) suggests hole transport deactivation at this field. This result is consistent with the finding of Juska *et.al*. [1, 14] who have shown by subnanosecond TOF method [15] that at ~ 50 V/μm hole drift mobility approaches the mobility of the free hole. However, the magnitudes of hole mobility (Fig. 4) are somewhat smaller than the corresponding values in a-Se monolayers [15] that can be attributed to the presence of potential barriers on CeO_2/a-Se and a-Se/ Sb_2S_3 interfaces.

Mobility deactivation at ~ 50 V/μm is apparently a precursor of impact ionization at higher fields. Indeed, further increase in the electric field leads to progressive hole heating that initiates avalanche multiplication at about 70 V/μm. This is accompanied by the abrupt changes in the shape of a photocurrent (Fig. 3) which starts to exhibit rapid burst due to the fast motion of avalanching holes and long tail due to the slower non-avalanching electrons. The absence of peaks in this tail suggests that electrons do not avalanche. The photocurrent ramp up time of ~ 1 ns indicates appropriate timing resolution for use in PET detectors.

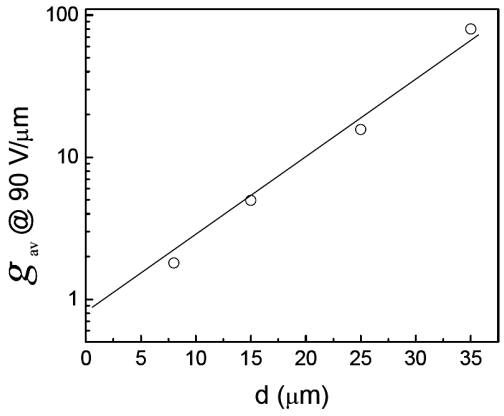

Figure 8 The dependence of hole avalanche multiplication gain g_{av} on a-Se HARP layer thickness d at electric field of 90 V/μm.

The straightforward evidence of just one type of carriers, namely, holes, that undergo avalanche multiplication is given in Fig. 8 where avalanche gain g_{av} shown in Fig. 6 is re-plotted *vs.* a-Se thickness d for a given electric field. The linear dependence of $\log(g_{av})$ *vs.* d proves that g_{av} depends on the sample thickness d as

$$g_{av} = \exp(\gamma_p d), \qquad (3)$$

where γ_p is the field depended impact ionization coefficient (IIC) for holes.

As it is seen from the Figures 6 and 8 the thicker the a-Se layer, the higher is the gain for a given electric field in full agreement with Eq. (3). Since g_{av} depends exponentially on d it is tempting to use thick a-Se layers in order to increase photosensor gain. This, however, will not furnish the desired result. The reason is that the thicker a-Se layer, the lower is the electric field F_{BR} at which electrons start to avalanche. As a result, a self-sustaining avalanche breakdown process is initiated and lasts till the total created charge screens the external bias. Thus, $F > F_{BR}$ can not be achieved. The criteria of F_{BR} is given by the equation (4) 4]:

$$(\gamma_n d + 1)\gamma_p - \gamma_n \exp(\gamma_p d) + \gamma_n = 0 \quad (4)$$

where γ_n is a field dependent IIC for electrons.

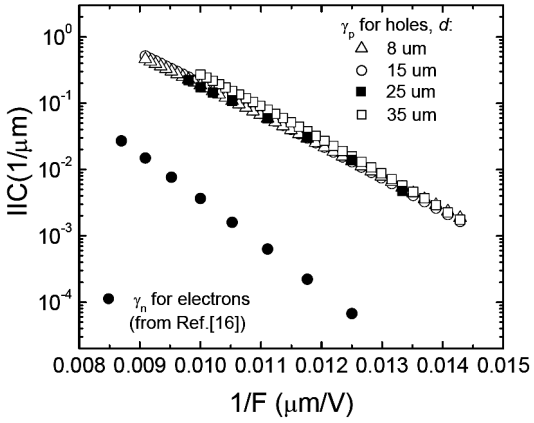

Figure 9 Experimentally determined impact ionization coefficients for both, holes and electrons plotted *vs.* reciprocal electric field.

Field dependences of γ_p were determined from the avalanche gain measurements using equation (3) (Fig. 9) while field dependences of γ_n were adopted from [4] since the HARP tube structure used here permits illumination only of the positive electrode and therefore the study of photogeneration and transport of holes only. Using $\gamma_p(F)$ and $\gamma_n(F)$ dependencies the appropriate F_{BR} was calculated numerically for given d to satisfy the condition (4). The resulting F_{BR} values for different a-Se layer thicknesses are shown in Fig. 7 by solid line. As it is seen from Figure 7 calculated values agree well with the experimentally found F_{BR}.

Based on the calculated F_{BR} maximum gain g_{MAX} was estimated as

$$g_{MAX} = \exp[\gamma(F_{BR})d] \quad (5)$$

by substituting corresponding $\gamma(F_{BR})$ (see Fig. 10).

While for comparatively thin a-Se layers (d < 35 μm) g_{MAX} sharply increases with thickness, it experiences a knee

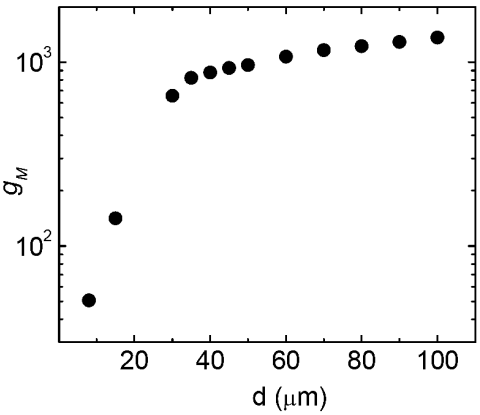

Figure 10 Maximal achievable multiplication gain for different a-Se layer thicknesses.

at d > 35 μm. Thus, for layers thicker than ~ 35 μm the increase in g_{av} due to increase in thickness is compensated by a decrease due to the constraint of the application of the lower field which cannot exceed F_{BR}. As a result the gain saturates. This suggests that d=35 μm should be considered as a practical limit for a-Se photosensor.

4 Conclusions We present experimental data on the evaluation of photoconductivity and hole transport in a-Se multilayers of HARP phototatgets that are first practical a-Se photodetectors utilizing avalanche multiplication gain. The results suggest that hole transport and avalanche formation mechanisms in a-Se HARP multilayers are similar to those previously found on a-Se monolayers confined between insulating films. Thus, incorporation of blocking layers for holes and electrons does not disturb photoconductive properties while provides constant photocurrent flow required for photosensor operation.

It was found that avalanche multiplication gain depends exponentially on layer thickness d reaching the value of 1000 for d =35 mm. Further increase in d however does not result in significant gain grows due to the decrease in maximum achievable electric field. The combination of high avalanche gain with extremely high quantum efficiency for blue light (~ 100%) and fast photocurrent response (1 ns) makes a-Se HARP layer a prospective material to use in combination with scintillation crystal in PET detectors.

Acknowledgements Financial support from the Susan G. Komen Breast Cancer Foundation (Grant # BCTR0504418), Cancer Care Ontario (CINO), and from the Deutsche Forschungsgemeinschaft is gratefully acknowledged.

References

[1] G. Juska and K. Arlauskas, phys. stat. sol. (a) **59**, 389 (1980).
[2] O. Rubel, S.D. Baranovskii, I.P. Zvyagin, and S.O. Kasap, phys. stat. sol. (c) **1**(5) 1186 (2004).

[3] A. Reznik, S.D. Baranovskii, O. Rubel, G. Juska, S.O. Kasap, Y. Ohkawa, K. Tanioka, and J.A. Rowlands, J. Appl. Phys. (in press).
[4] A. Cesnys, G. Juska, and E. Montrimas, in: Semiconducting Chalcogenide Glass II: Properties of Chalcogenide Glasses, edited by R. Fairman and B. Ushkov (Elsevier Academic Press, 2004), p. 15.
[5] E. Maruyama, Jpn. J. Appl. Phys. **21**, 213 (1992).
[6] M. Kubota, T. Kato, S. Suzuki, H. Maruyama, K.Shidara, K. Tanioka, K. Sameshima, T. Makishima, K. Tsuji, T. Hirai, and T. Yoshida, IEEE Trans. Broadcasting **42**(3), 251 (1996).
[7] K Tanioka, J. Yamzaki, K. Shidara, K. Taketoshi, T. Kawamura, T. Hirai, and Y. Takasaki, Adv. Electron. Electron Phys. **74**, 379 (1998).
[8] W. Zhao, D. Li, A. Reznik, B.J.M. Lui, D.C. Hunt, Y. Ohkawa, K. Tanioka, and J.A. Rowlands, Med. Phys. **32**(9), 2954 (2005).
[9] A. Reznik, B.J. M. Lui, and J.A. Rowlands, Technol. Cancer Res.Treatm. **4**, 61 (2005).
[10] W.-D. Park and K. Tanioka, Jpn. J. Appl. Phys. **42**, L209 (2003).
[11] A. Reznik, B.J. M. Lui, Y. Ohkawa , T. Matsubara, K. Miyakawa, M. Kubota, K. Tanioka, T. Kawai, W. Zhao, and J.A. Rowlands, Nucl. Instrum. Methods Phys. Res. A **567**, 93 (2006).
[12] T. Ohshima, K. Tsuji, K. Sameshima, T. Hirai, K. Shidara, and K. Taketoshi, Jpn. J. Appl. Phys. **30**, L1071 (1991).
[13] S. Kasap, J.A. Rowlands, S.D. Baranovskii, and K. Tanioka, J. Appl. Phys., **96**(4), 2037 (2004).
[14] G. Juska and K. Arlauskas, phys. stat. sol. (a) **77**, 387 (1983).
[15] G. Juska, J. Non-Cryst. Solids **137**/**138**, 410 (1991).